Novel Strategy for Finding the Optimal Parameters of Ion Selective Electrodes

J. J. Jasielec[a], B. Wierzba[b], B. Grysakowski[b], T. Sokalski[a], M. Danielewski[b]
and A. Lewenstam[a,b]

a) Laboratory of Analytical Chemistry and Centre for Process Analytical Chemistry and
Sensor Technology 'ProSens', Process Chemistry Centre, Åbo Akademi University,
Biskopsgatan 8, 20500 Åbo, Finland
b) Interdisciplinary Centre for Materials Modelling, FMS&C, AGH University of Science
and Technology, Al. Mickiewicza 30, 30-059 Cracow, Poland

The detection limit (DL) of an analytical method determines the range of its applicability. For ion selective electrodes (ISE) used in potentiometric measurements, this parameter can vary by several orders of magnitude depending on the inner solution concentrations or the time of measurement. The detection limit of ISE can be predicted using the Nernst-Planck-Poisson model (NPP), as a general approach to the description of the time-dependent electro-diffusion processes. To find the optimal parameters, we need to formulate the inverse electro-diffusion problem. In this work, we combine the Nernst-Planck-Poisson model with the Hierarchical Genetic Strategy with real number encoding (HGS-FP). We use the HGS-FP method to approximate inner solution concentrations as well as the measuring time that provide a linear dependence of the membrane potential over the widest concentration range. We show that the HGS-FP method allows us to find the solution of the inverse problem. The presented calculations show a great future potential of the NPP method combined with the HGS-FP strategy.

Introduction

Ion Selective Electrodes (ISE)

ISEs are potentiometric sensors very commonly used in chemical analysis especially in the area of clinical and environmental applications. The most import parameters of ISE are the selectivity coefficient (Kij) and detection limit (L) (1)

Detection limit of ISEs can be engineered to vary by several orders of magnitude depending on the inner solution concentrations (2) or the time of measurement (3).

Nernst-Planck-Poisson Model (NPP)

There are many models describing the response of ISEs. They differ in generality and idealization level. So far the Nernst-Planck-Poisson (NPP) is the most general (1).

The application of the NPP model to membrane electrochemistry was presented in a seminal paper (4). The authors developed an efficient finite difference scheme, totally implicit in time. The resulting set of non-linear algebraic equations was solved using the Newton-Raphson method.

An approach, based upon this idea and dedicated to the general description of ISE behaviour, was later developed (3, 5-7).

The first extension of the NPP model for a two layer system was presented in (8). The first NPP model implementation where the method of lines (MOL) was used was presented in (9, 10). Later on, MOL extensions of the NPP model for an arbitrary number of layers were developed and implemented in C++ (11) or in MathCad (3) and Matlab (12) scripts.

<u>NPP Short Description</u>

The Nernst-Planck-Poisson model is an initial-boundary value problem that for one dimension is given by the set of equations given below. The system consists of n (2 in this particular case) layers, one representing the diffusion layer of aqueous solution and one that represents the membrane. Each layer has its own thickness d^j and dielectric permittivity ε^j, is flat and isotropic, so it can be considered as a continuous environment inside which the change in space and time of concentration of r components c_i^j and of electric field E^j takes place. This system is presented in Fig. 1.
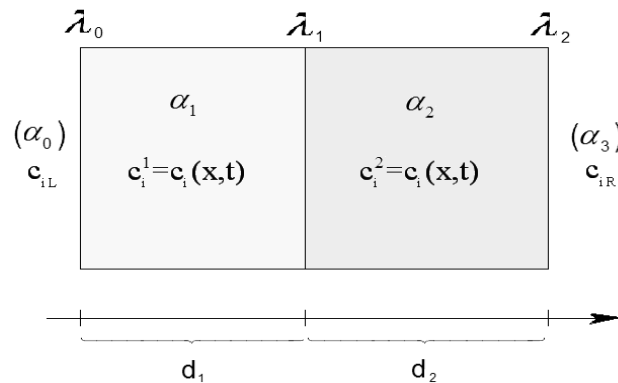

Figure 1. Scheme of a 2-layer system between two solutions. c_{iL} and c_{iR} is the concentration of the i-th component in the solution on the left and right side, respectively.

The ionic fluxes are expressed by Nernst-Planck equation:

$$J_i^j(x,t) = -D_i^j \left[\frac{\partial c_i^j(x,t)}{\partial x} + \frac{F}{RT} z_i c_i^j(x,t) E^j(x,t) \right] \qquad [1]$$

where: $J_i^j(t,x)$ is the flux of the i-th ion in the j-th layer, D_i^j is the constant self diffusion coefficient of the i-th ion in the j-th layer, $c_i^j(t,x)$ is the concentration of i-th ion in the j-th layer, z_i the valence of i-th ion, and $E^j(t,x)$ is electric field in the j-th layer. F is Faraday constant, R and T denote the gas constant and absolute temperature.

The evolution of the electric field is represented by the Poisson equation:

$$\frac{\partial E^j(t,x)}{\partial x} = \frac{\rho^j(t,x)}{\varepsilon^j} \qquad [2]$$

where:

$$\rho^j(t,x) = F \sum_i^n z_i c_i^j(t,x) \qquad [3]$$

denotes the charge density. The mass conservation law describes the evolution of concentrations:

$$\frac{\partial c_i^j(t,x)}{\partial t} = -\frac{\partial J_i^j(t,x)}{\partial x} \qquad [4]$$

In this work, the Poisson equation is replaced by its equivalent form, the total current equation(13):

$$I(t) = F\sum_i^n z_i J_i^j(t,x) + \varepsilon^j \frac{\partial E^j(t,x)}{\partial t} \qquad [5]$$

The values of fluxes at the boundaries (the interface λ_j between layers α_j and α_{j+1}) are calculated using modified Chang-Jaffe conditions (14) in the form:

$$J_i^j(\lambda_j,t) = J_i^{j+1}(\lambda_j,t) = \overrightarrow{k_{i\lambda_j}} c_i^j(\lambda_j,t) - \overleftarrow{k_{i\lambda_j}} c_i^{j+1}(\lambda_j,t) \qquad [6]$$

where $\overrightarrow{k_{i\lambda_j}}, \overleftarrow{k_{i\lambda_j}}$ are the first order heterogeneous rate constants used to describe the interfacial kinetics. The $\overrightarrow{k_{i\lambda_j}}$ constant corresponds to the ion i, which moves from layer α_j to α_{j+1}, and $\overleftarrow{k_{i\lambda_j}}$ - to the ion i, which moves from α_{j+1} to α_j.

The boundary points x = λ_j are specific points special points which have a neighbourhood in two different layers. Because of this fact two values of each ion concentration, ($c_i^j(\lambda_j,t)$ and $c_i^{j+1}(\lambda_j,t)$) as well as two of electrical field values ($E^j(\lambda_j,t)$ and $E^j(\lambda_j,t)$), should be considered.

Initial concentrations fulfil the electro-neutrality condition and, consequently, there is no initial space charge in the membrane (7):

$$c_i^j(0,x) = c_{Mi}^j(x), \qquad E^j(0,x) = 0 \qquad for \quad x \in [0,d] \qquad [7]$$

The membrane potential, $\phi(t)$, is obviously given by:

$$\phi(t) = -\int_0^{d_1} E^1(t,x)\,dx - \int_{d_1}^{d_2} E^2(t,x)\,dx \qquad [8]$$

Detection Limit – Inverse Problem

It is well known from the abundant literature data that a gradual decrease in the concentration of the main ion in the inner solution of a plastic membrane ISE leads to the improvement (decrease) of the detection limit. However, when the concentration of the main ion in the inner solution becomes too low, a super-nernstian behaviour, due to the over-compensation of the trans-membrane fluxes of ions, is observed. This phenomenon is presented in Fig. 2. All the physical properties of ions and other parameters used in simulations are given in Appendix A.
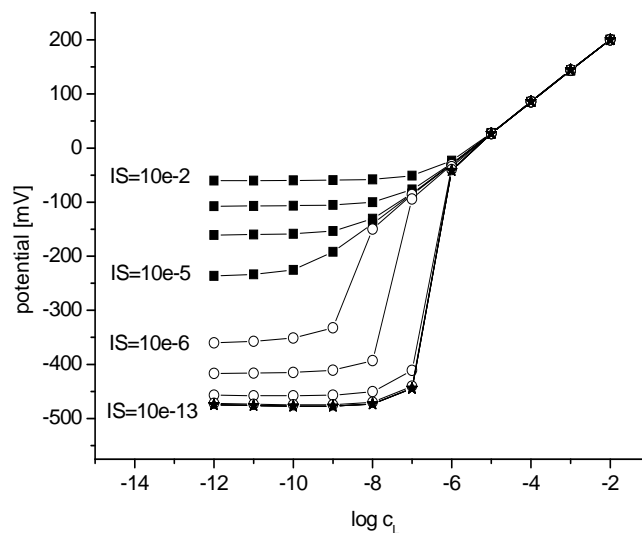
Figure 2. Influence of the concentration of the preferred ion in the inner solution (15)

If the measuring time is too short (t<300s) to allow steady-state to be achieved, it will affect the potential, i.e. the shape of the calibration curve. An ISE with a preferred ion concentration in the internal solution equal to 10^{-6}M (ISE6) was used to illustrate this phenomenon (Fig. 3).
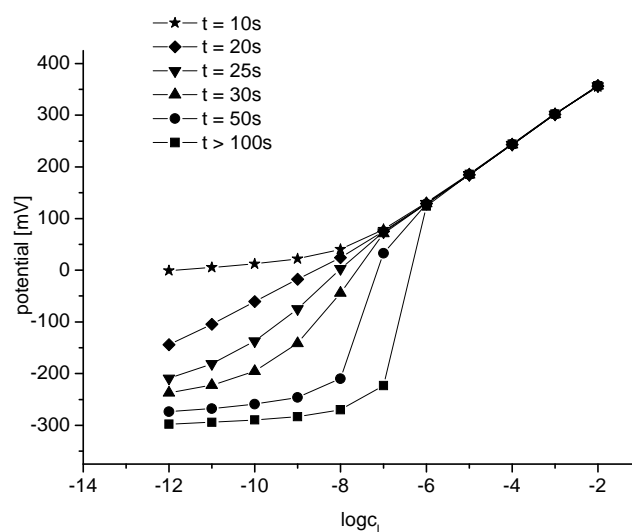

Figure 3. Influence of measuring time for the ISE with preferred ion inner solution concentration 10^{-10} M (15).

At first, with increasing measuring times (t), the detection limit decreases. A further increase of t causes the appearance of a super-nernstian section, or jump, in the calibration curve. The longer the measuring time becomes, the more this jump moves toward higher concentrations, thus increasing the detection limit

The cases described above are of the "normal problem" type ("What is the value of the detection limit if we have a certain set of parameters?"). Equally, or maybe more,

important is the so called "inverse problem" namely "Which set of parameters produces the best detection limit?"

The answer to this problem is illustrated in Fig. 4 which shows contour plot of the detection limit vs. the measurement time and the concentration of the preferred ion in the inner solution (DL-t-[I]).
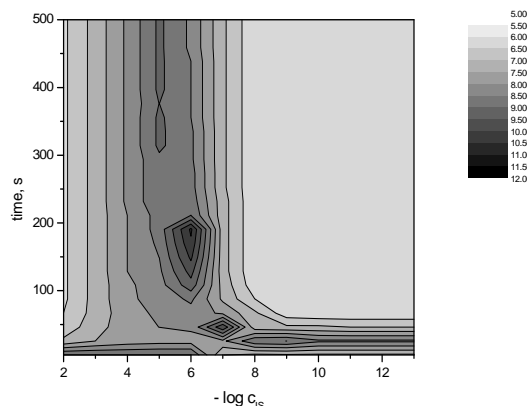

Figure 4. The time-concentration-detection limit map obtained using the NPP mode l(15).

The concentration of I is plotted on the x-axis, the measuring time on the y-axis and the resulting value of the detection limit on the z-axis. The detection limit is depicted with the help of different colour intensities; the darker the colour, the lower the detection limit. The local/global minima can be read from the plot.

In order to obtain such contour plots, the measuring time was increased from 5 to 500 seconds with an interval of 5s, and the ion concentration in the inner solution was varied over a range of ten orders of magnitude (10^{-2}-10^{-12} M) with an interval of one order of magnitude. For each calibration curve, 11 points were calculated. Thus, 100x12 = 1200 calibration curves and altogether 13 200 points had to be calculated. The total calculation time was 15 days. This is a "brute force" approach that requires a lot of computational effort, which is exponentially proportional to the number of investigated parameters.

Hierarchical Genetic Strategy with Real Number Encoding (HGS-FP) (16).

The genetic algorithms are highly efficient in solving problems with many optima (17, 18). The HGS introduced in 2000 (19) is one such efficient algorithm. The ability of this algorithm to find optima (maxima or minima) efficiently, i.e. at low computational cost, is due to the concurrent search inside the optimization space by small populations of individuals (solutions). The creation of these populations is governed by genetic processes with low complexity. HGS was further generalized (16) by introduction of the floating point encoding (HGS-FP). The real number encoding used in HGS-FP is much more efficient than the normally used binary encodings (0,1 codes) due to the conservation of the natural (topological) space where all variables are real numbers.

The HGS accuracy and low computational cost for multimodal benchmarks was shown in (16) (20)

The main engine of the HGS-FP is running a set of evolutionary processes (21, 22). The algorithm in each evolving step creates a new population which is searched for optima.

Let $\Im = [a,b]^N \subset \mathbf{R}^N$ denote the fitness function domain (goal function domain). N is the dimension of the problem (number of variables) and a, b are the left and right boundaries of the search space (goal function domain or optimization space), respectively. The two genetic operators for floating point representation are given by:

1) crossover (generation of a new individual from two already existing ones):

$$Y_i = X_i^1 + \mathcal{N}(mean, \sigma)(X_i^2 - X_i^1), \quad i = 1,...,N \qquad [9]$$

2) mutation (generation of a new individual from the already existing one):

$$Y_i = X_i^1 + (\mathcal{N}(0, \sigma))_i, \quad i = 1,...,N \qquad [10]$$

where: Y_i is a new individual generated by crossover or mutation, X_i^1 and X_i^2 are parents individuals, $\mathcal{N}(mean, \sigma)$ denotes the normally distributed random variable, where $mean$ is a random number and σ its variation.

For a new population to be produced, the classical roulette selection is used. The probability, $\Pr(X)$, of obtaining an individual X from the population P, ($X \in P$) is:

$$\Pr(X) = \frac{fitness(X)}{\sum_{Y \in P} fitness(Y)}, \quad \forall X \in P \qquad [11]$$

where: $fitness(X)$ is an estimation of the adaptation of the X–th individual (the value of goal function)

As an example, the results obtained with HGS-FP method for the 2-dimensional test function (23) ($f(x,y) = \cos(5\pi x) + \cos(5\pi y) + x^2 + y^2, \quad x, y \in [-0,7; 0,7]$) are shown in Fig. 5. This function is generally accepted test function used to compare and evaluate different algorithms. The objective was to find all of the function maxima. The dots in the Fig. 5 denote the position (x_i, y_i) of each of the individuals in the search space.
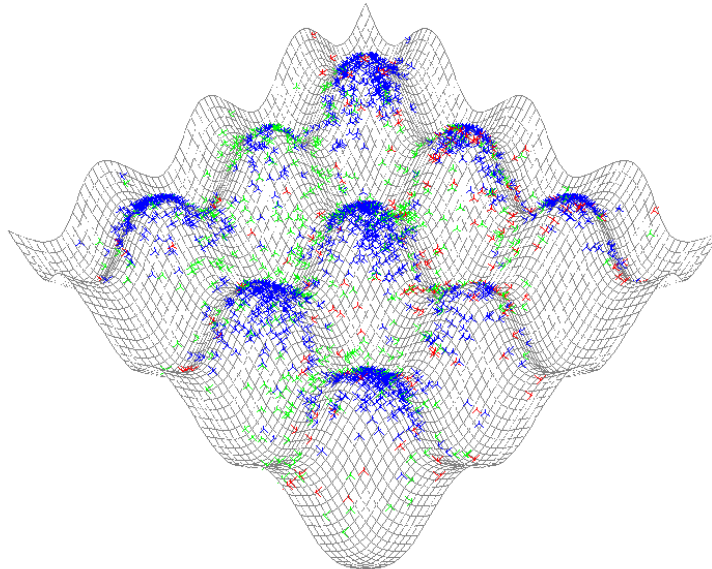

Figure 5. The results of searching for maxima for a standard test function with the HGS-FP method. Dots show the positions of individuals in the search space. The red, green and blue colours denote the individuals of the first, second and third populations, respectively.

The correctness of the HGS-FP strategy was also checked in the case of the 20-dimensional test functions (16). In all cases the HGS-FP found the global extreme more quickly and accurately than, like Simple Genetic Algorithm (SGA), Genitor and many others (16, 20).

Results and Discussion

Applying the HGS-FP strategy in order to find the optimal parameters we reformulated the NPP problem into the optimization one (finding the extreme). The problem is to find the concentration of the preferred ion in the inner solution and the measuring time providing the best detection limit of an ISE.

Figure 6 shows the time-concentration-detection limit map obtained using the NPP model (see Fig. 4) with overlaid points obtained with NPP-HGS method

The NPP-HGS algorithm was able to find all the minima on the map. It needed to calculate only 214 calibration curves in order to achieve this task. The computational effort was around 6 times smaller compared with the "brute force" approach.
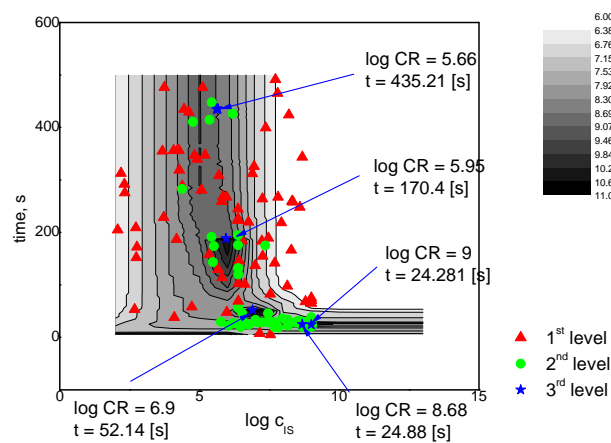

Figure 6. Time concentration map with all the individuals (points) of HGS. The red, green and blue colours denote the individuals of the first, second and third populations, respectively.

To further demonstrate the effectiveness of NPP-HGS method the optimization of three parameters (concentration of the primary ion in the inner solution, measuring time, and diffusion coefficient of the preferred ion in the membrane) was made. The results are presented in Fig. 7.
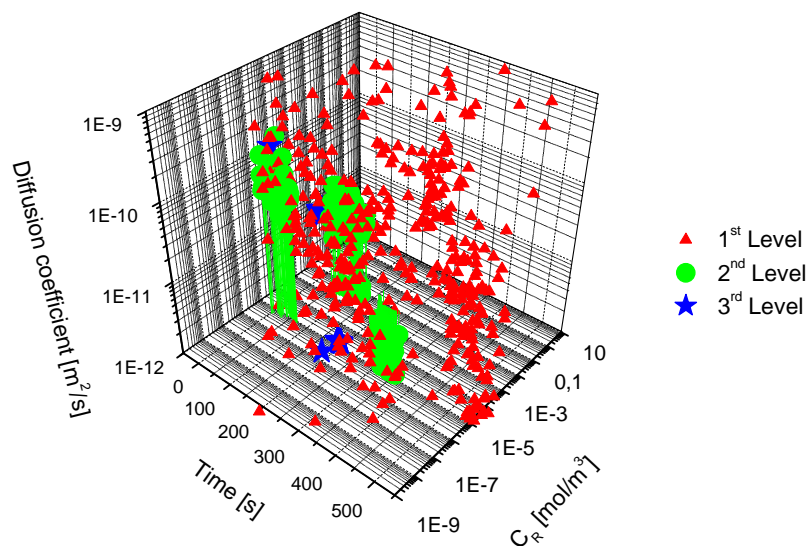
Figure 7. The individuals (points) of HGS in $(D_1, c_{1R}, \text{time})$ space. The red, green and blue colours denote the individuals of the first, second and third populations, respectively.

They show that the lowest detection limit is obtained in two regions:

1) $\log(c_{DL}) < -11.5$ when the diffusion coefficient of the preferred ion is in the range $5.1 \cdot 10^{-11}$ to $5.9 \cdot 10^{-11}$ m^2/s, its internal solution is in the range $8.8 \cdot 10^{-9}$ to $9.6 \cdot 10^{-9}$ M and measuring time is around 27 s.

2) $\log(c_{DL}) < -10.5$ when the diffusion coefficient of the preferred ion is in the range $1.0 \cdot 10^{-11}$ to $1.2 \cdot 10^{-11}$ m^2/s, its internal solution is in the range $2.2 \cdot 10^{-6}$ to $2.4 \cdot 10^{-6}$ M and measuring time is around 482 s.

This result would be very unfeasible to obtain by the brute force approach. We would have to calculate 12 000 calibration curves (132 000 points) which would take around 150 days. The computational effort using NPP-HGS method was around 20 times smaller compared with the "brute force" approach. The parallel version of HGS allows for further decrease of the computation time (22).

Conclusions

The NPP model is the most rigorous, complete and general from all models introduced to describe open-circuit membrane potential. The NPP allows direct prediction of the response of ion-selective membrane electrodes over space and time, including the propagation of selectivity and detection limit over time. As the least arbitral model from all used so far it makes possible solving inverse problems with a given target.

We showed how to combine the Hierarchical Genetic Strategy with real number encoding (HGS-FP) and the Nernst-Planck-Poisson (NPP) model. The NPP-HGS method was used to solve the inverse problem i.e. to find the optimal parameters for achieving the best detection limit of an ISE. The results in the case of two parameter optimization were compared with those obtained by the brute force approach. The agreement was good and

the computational effort much smaller for the NPP-HGS method. The gain in computational time was even bigger in the case of three parameter optimization. The presented results show potential of HGS-FP strategy.

The HGS-NPP method could be used for solving problems related to the analytical applications of ISEs. In particular, the advantages of time dependent selectivity and/or detection limit can be exploited, disadvantages of poor response can be diagnosed and avoided or optimized design of ISEs can be undertaken.

Acknowledgements

Appendix A. Simulation data

Data used in simulations are: thickness of the layers: $d_1 = 100$ and $d_2 = 200 \, \mu m$, absolute temperature: 298.16 K. Properties of ions are given in the below table

Table 1. The ion properties used in simulations:

	Ion 1	Iont 2	Iont 3	Ion 4
$D_i^1 \left[m^2 \cdot s^{-1} \right]$	$1.98 \cdot 10^{-9}$	$2.01 \cdot 10^{-9}$	$1.36 \cdot 10^{-9}$	$1.0 \cdot 10^{-9}$
$D_i^2 \left[m^2 \cdot s^{-1} \right]$	$1.98 \cdot 10^{-11}$	$2.01 \cdot 10^{-11}$	$1.36 \cdot 10^{-11}$	$1.0 \cdot 10^{-11}$
z_i	1	-1	1	-1
$c_L [M]$	1	1	10^{-7}	0
$c_M{}^1 [M]$	0.01	0.01	10^{-7}	0
$c_M{}^2 [M]$	0.0001	0	0	0.0001
$c_R [M]$	optimized	100.1	100	0
$\overrightarrow{k_{i\lambda_0}} \left[m \cdot s^{-1} \right]$	100	100	100	0
$\overrightarrow{k_{i\lambda_1}} \left[m \cdot s^{-1} \right]$	100	0.001	10^{-5}	0
$\overrightarrow{k_{i\lambda_2}} \left[m \cdot s^{-1} \right]$	100	100	100	0
$\overleftarrow{k_{i\lambda_0}} \left[m \cdot s^{-1} \right]$	100	100	100	0
$\overleftarrow{k_{i\lambda_1}} \left[m \cdot s^{-1} \right]$	100	100	100	0
$\overleftarrow{k_{i\lambda_2}} \left[m \cdot s^{-1} \right]$	100	0.001	10^{-5}	0

References

1. J. Bobacka, A. Ivaska and A. Lewenstam, *Chem. Rev.*, **108**, 329-351(2008).
2. T. Sokalski, A. Ceresa, T. Zwickl and E. Pretsch, *J. Am. Chem. Soc.*, **119**, 11347-11348(1997).
3. T. Sokalski, W. Kucza, M. Danielewski and A. Lewenstam, *Anal. Chem.*, **81**, 5016-5022(2009).
4. T. R. Brumleve and R. P. Buck, *J.Electroanal.Chem.*, **90**, 1-31(1978).
5. P. Lingenfelter, I. Bedlechowicz-Sliwakowska, T. Sokalski, M. Maj-Zurawska and A. Lewenstam, *Anal. Chem.*, **78**, 6783-6791(2006).
6. T. Sokalski and A. Lewenstam, *Electrochem.Commun.*, **3**, 107-112(2001).
7. T. Sokalski, P. Lingenfelter and A. Lewenstam, *J.Phys.Chem.B*, **107**, 2443-2452(2003).
8. P. Lingenfelter, T. Sokalski and A. Lewenstam, Matrafured, Hungary, 2005.
9. R. Filipek, *Polish Ceramic Bulletin*, **90**, 103-108(2005).
10. W. Kucza, M. Danielewski and A. Lewenstam, *Electrochem. Commun.*, **8**, 416-420(2006).
11. J. Jasielec, AGH-UST/AAU, 2008.
12. B. Grysakowski, B. Bozek and M. Danielewski, *Diffusion in Solids and Liquids III*, **273-276**, 113-118(2008).
13. H. Cohen and J. W. Cooley, *Biophys. J.*, **5**, 145-162(1965).
14. H. C. Chang and G. Jaffe, *J. Chem. Phys.*, **20**, 1071-1077(1952).
15. J. J. Jasielec, T. Sokalski, R. Filipek and A. Lewenstam, *Electrochim. Acta*, **55**, 6836-6848(2010).
16. A. Semczuk and B. Wierzba, Krakow, Jagiellonian University, Institute of Computer Science, Master of Science thesis (in polish), 2003.
17. Cantu-Paz E.; *Efficient and Accurate Parallel Genetic Algorithms*. Kluwer Academic Publishers, Norwell, MA, 2000.
18. Cabib, E., Schaefer, R., Telega, H.: A Parallel Genetic Clustering for Inverse Problems. In: KĺgstrÖm, B., Elmroth, E., Waśniewski, J., Dongarra, J. (eds.) PARA 1998. LNCS, vol. 1541, pp. 551–556. Springer, Heidelberg (1998)
19. Kolodziej J., Gwizdala R., Wojtusiak J. : Hierarchical Genetic Strategy as a Method of Improving Search Efficiency, *Advances in Multi-Agents Systems* , R Schaefer and S. Sedziwy eds.,UJ Press, **7**, 149-161(2000).
20. Kolodziej J.: *Modelling Hierarchical Genetic Strategy as a Family of Markov* Chains**,** R. Wyrzykowski et al. (Eds.): PPAM 2001, LNCS 2328, pp. 595–598, 2002. Springer-Verlag Berlin Heidelberg 2002
21. R. Schaefer and B. Barabasz, *Asymptotic Behavior of* **hp***–HGS (***hp***-Adaptive Finite Element Method Coupled with the Hierarchic Genetic Strategy) by Solving Inverse Problems*, M. Bubak et al. (Eds.): ICCS 2008, Part III, LNCS 5103, pp. 682–691, 2008. Springer-Verlag Berlin Heidelberg 2008
22. J. Kolodziej, R. Schaefer and A. Paszynska, *Journal of Theoretical and Applied Mechanics, Computational Intelligence*, **42**, 519-539(2004).
23. R. Salomon, *Biosystems*, **39**, 263(1996).